

THE USE OF FAST FACTORISED BACK PROJECTION FOR SYNTHETIC APERTURE SONAR IMAGING

S.M. Banks

University College London, Department of Electronic and Electrical Engineering

H. D. Griffiths

University College London, Department of Electronic and Electrical Engineering

1. INTRODUCTION

Synthetic Aperture Sonar (SAS) provides a large improvement in azimuth resolution compared to conventional side-scan sonar; the azimuth resolution is also independent of range. This improvement is achieved by combining the data from a number of pings to synthesise a long virtual receive array. Synthetic aperture imaging techniques have been applied to both space and aircraft borne Synthetic Aperture Radar (SAR) for several decades, an early patent on the technique being [9]. Probably the first application to sonar followed some years after [10], however the development of synthetic aperture sonar has been slow compared to the equivalent radar systems.

A number of techniques for forming images from synthetic aperture data (inversion) have been developed for both radar and sonar. Exact inversion in the time domain is possible for a general aperture geometry however the computational burden is very high (normally an $O(N^3)$ process). The large computation times needed for exact time domain inversion can be avoided by using one of a number of frequency domain techniques such as the Chirp Scaling[1] or Range Doppler[2] algorithms. Frequency domain techniques generally work well if the synthetic aperture is evenly sampled and linear. Deviations from a linear, evenly sampled synthetic aperture that occur in sonar data can be shown to seriously degrade the image produced. Corrections can be made to the data prior to frequency domain inversion to compensate for motion errors, however these corrections do not always work, especially in the situation where the transmitter and receiver beamwidths are very broad and the motion errors are large. The frequency domain techniques also offer little flexibility in terms of choosing the area and resolution of the scene to be imaged and present a number of problems for real time systems.

A number of time domain techniques have been developed with complexities less than $O(N^3)$ such as the two stage method proposed in [6] and the method described in [7] based on a tomography algorithm. These work for a general aperture geometry and can form images of given areas of the target scene at any given resolution. The inversion technique described in this paper, Fast Factorised Back Projection (FFBP) is a fast time domain inversion technique developed recently for SAR [3]. An approximation used by FFBP can be varied allowing image quality to be traded with computation time. FFBP can produce images in a similar time to the Fourier based techniques using only a small approximation, hence negligible image degradation, however does not have the constraint of requiring a linear equispaced synthetic aperture. Because it can process the image a ping at a time it is highly suitable for application to a real time imaging system; it is also suited to implementation on parallel architectures.

FFBP is a phase preserving inversion method and is therefore suitable for producing interferometric sonar images. Interferometry allows 3D information about a scene to be derived from the phase difference between two images of the target scene formed using vertically separated receivers[11].

This paper discusses the application of FFBP to synthetic aperture sonar, and presents results achieved by applying the technique to real experimental data. The paper looks at the problem of SAS inversion from the point of view of applying radar techniques to sonar.

2. MOTIVATION

This work involves the development of processing algorithms for rail mounted, towed array and autonomous vehicle SAS systems. The SAS systems used in this work^[1] consist of broad beamwidth transmitters (around $\pm 20^\circ$) and multi-channel receiver arrays (sometimes called vernier arrays). The echo returns at each of the receivers are recorded separately. A similar set-up is commonly used in SAR, with the exception that the channels are usually summed in hardware to form a narrow beam and only the sum of the channels recorded^[2]. Recording the channels separately has the advantage that physical images of the scene can be formed from each ping and the synthetic aperture can be formed from the individual channels as opposed to forming a beam at each ping. Forming the synthetic aperture in this way is preferable to forming beams at each ping, and can be considered to be roughly equivalent to using spotlight mode processing for all areas in the scene. Extra consideration must be applied to motion compensation and spatial sampling when forming the synthetic aperture in this way; this is discussed in the next section. FFBP is a suitable method for forming SAS images in the presence of motion errors by using the individual hydrophones to form the synthetic aperture. The computation times are on a par with, or faster than, other algorithms in the literature with the added benefit of flexibility.

3. SYNTHETIC APERTURE INVERSION

This section describes the basic process of synthetic aperture inversion by looking at the exact time domain inversion technique applied to SAS. Most Fourier based techniques can be considered to perform inversion in the same manner, but exploit the fast Fourier transform to speed up the implementation of the discrete form of the inversion integral.

The process of collecting synthetic aperture sonar data is shown in figure 1. A platform consisting of a transmitter and receiver array is moved past the target scene. Pings are transmitted at regular intervals and the echo returns from the target scene recorded. The pulse repetition interval of the pings is chosen such that some of the phase centres^[3] from the current ping overlap some of those from the previous ping; this permits the application of motion compensation methods such as DPCA [4] and also ensures the aperture is adequately sampled.

If the azimuth sampling is considered to be continuous, the inversion process in the (x,y) plane for an infinite synthetic aperture is described by (1) (the inversion integral) where the image $I(x,y)$ is formed by inverting the raw data $R(r,y)$. $r_y(x,y)$ is the range from the transmit / receive phase centre at y' to the point (x,y) in the target scene given by (2) where p and q are the distances shown in figure 1. The distance along the synthetic aperture is y' .

$$I(x,y) = \int_{-\infty}^{\infty} R(r_y(x,y), y') dy' \quad \dots(1)$$

$$r_y(x,y) = \sqrt{p^2 + q^2} \quad \dots(2)$$

```

Title:
SonifyEps
Creator:
fig2dev Version 3.2 Patchlevel 10-beta3
Preview:
This EPS picture was not saved
with a preview included in it.
Comment:
This EPS picture will print to a
PostScript printer, but not to
other types of printers.

```

Figure 1 The SAS system imaging a scene

3.1 INVERSION OF DISCRETE DATA

The actual sonar data is discretely sampled over a finite synthetic aperture. The azimuth sampling is not evenly spaced; for example in figure 1 the azimuth sampling in areas where phase centres from adjacent pings overlap is, on average, twice that of areas of no overlap. The integration in (1) is implemented, in this work, for the discrete case using the trapezoidal rule. Other more accurate forms of numerical integration such as Simpson's rule could be used at the expense of increased computation time. (1) is rewritten in the discrete case in (3) for N sampled data lines

$$I(x, y) = \frac{1}{2} \left[b_1 R(r_1(x, y), 1) + \sum_{n=2}^{N-1} (b_{n-1} + b_n) R(r_n(x, y), n) + b_{N-1} R(r_N(x, y), N) \right] \quad \dots(3)$$

where b_n is the azimuth distance between the sampling positions of $R(r_n, n)$ and $R(r_{n+1}, n+1)$ along the aperture divided by the mean spacing \bar{d} . The azimuth sampling position y' is replaced with the sampled data line n . The numerical integration process is shown in figure 2

```

Title:
Integration.eps
Creator:
fig2dev Version 3.2 Patchlevel 10-beta3
Preview:
This EPS picture was not saved
with a preview included in it.
Comment:
This EPS picture will print to a
PostScript printer, but not to
other types of printers.

```

Figure 2 Numerical integration of non evenly sampled aperture

The number of operations required to implement (3) is $O(N^3)$ for an image with $N \times N$ pixels formed from an aperture with N azimuth samples. This very high complexity is reduced in this work by the use of FFBP (discussed in a later section).

It is common practice to perform the inversion using a complex baseband version of the analytic form of the raw sonar data. The analytic form of a signal is obtained by summing the signal with its Hilbert transform [8]. When using complex basebanded data each term in (3) must be multiplied by the phase term $e^{j2\omega_c r_n(x,y)}$ where ω_c is the centre angular frequency of the original pulse function. (3) can be re-written as (4) for the complex baseband case.

$$I(x,y) = \frac{1}{2} \left[b_1 R(r_1(x,y), 1) e^{j2\omega_c r_1(x,y)} + \left[\sum_{n=2}^{N-1} (b_{n-1} + b_n) R(r_n(x,y), n) e^{j2\omega_c r_n(x,y)} \right] + b_{N-1} R(r_N(x,y), N) e^{j2\omega_c r_N(x,y)} \right]$$

...(4)

3.2 DEVIATIONS FROM A LINEAR APERTURE

Many synthetic aperture inversion techniques assume the synthetic aperture is linear. Corrections for a non linear aperture are sometimes made by applying delays to the raw sonar data to make it appear that it was sampled from a linear aperture. This subsection shows that such a correction is valid for small motion errors and narrow beamwidths (as may be the case if beamforming along the receive array were performed at each ping) but is not valid when individual hydrophones, with a broad beamwidth, are used and when the motion errors are not small. Figure 3 shows the source of this error. Two points, P1 and P2, are imaged from a transmit / receive phase centre at position R'. The ideal position of the phase centre is at R, a distance d away from R' in the x direction. The returns from point P1 can be corrected to make it appear that the phase centre was at R by delaying the data by $2d/c$ where c is the speed of sound. Such a correction is exact for P1 (excluding amplitude changes) however is approximate for reflections from point P2. (5) gives the two way error, e , between d and the correction required to accurately correct for the returns from point P2, initially a distance r away and at an angle Φ .

$$e = 2 \left\{ r - d - \sqrt{r^2 - 2dr \cos(\Phi) + d^2} \right\} \quad \dots(5)$$

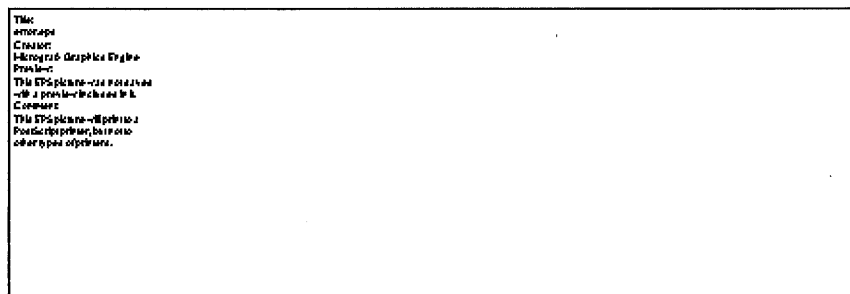


Figure 3 Error introduced by correcting raw data

The error should be kept within half a wavelength (λ) of the two way travel distance (i.e. $e < \lambda/2$) to avoid significant image degradation. For a beamwidth of $\pm 20^\circ$, a motion correction of $d = 0.05\text{m}$ and a scene $r=70\text{m}$ away the error introduced for P2 by correcting the raw data using a delay is $e=0.006\text{m}$. For the system used in this work, the wavelength of the centre frequency of the ping is $\lambda=0.01\text{m}$ making the error $\lambda/1.66$, higher than the required maximum of $\lambda/2$. Reducing the beamwidth to $\pm 5^\circ$ (e.g. by beamforming at each ping) the error becomes $\lambda/26$, i.e. within the required accuracy.

Although the motion errors are smaller than 0.05m in the rail mounted data used in this work (and presented here) motion errors present in data from autonomous vehicles can be more than 10 times this value. Motion correction is therefore not be done by correcting the raw data, but is carried out by taking account of the true position of the phase centre in the inversion equation, (4), i.e. calculating the range r from the true position, not correcting the data and calculating the range from the corrected position. In this way the synthetic aperture inversion process can accommodate a general aperture geometry.

4. FAST FACTORISED BACKPROJECTION

It has been shown that exact time domain inversion is highly suited to the synthetic aperture system used in this work, however the high computational complexity $O(N^3)$ makes the computation times prohibitively long, especially for any future implementation in a real time system. FFBP can be used to vastly speed up the inversion at the expense of adding a variable approximation. The approximation can be changed allowing image quality to be traded for lower computation time. This section describes, briefly, the process of fast factorised back projection (FFBP). The method, recently developed for SAR, is described more comprehensively in [3], [5] and [12].

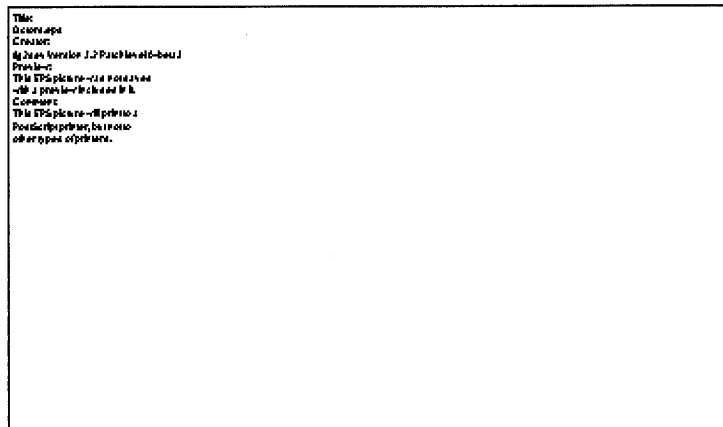


Figure 4 The factorisation process used in FFBP

Instead of projecting all the raw data to every pixel in the final image, FFBP arrives at the final image via a variable number of intermediate stages. Each intermediate stage involves forming an increasing number of polar images from progressively fewer (and larger) 'sub-apertures'. An example of the factorisation process for 3 stages is shown in figure 4. In each stage polar images centred on the crosses shown are formed from the elements in the each of the sub apertures. The number of operations required in each stage is given by (6) where N_{saps} is the number of sub-apertures, N_{sapels} is the number of sub apertures from the previous stage in each sub aperture of the current stage, R_{pixels} is the number of range pixels in each polar sub image and S_{imgs} is the number of sub-images.

$$O = N_{saps} * N_{sapels} * R_{pixels} * S_{imgs} \quad \dots(6)$$

[3] shows that so long as the range error $|\Delta R|_{max}$ at the edge of each sub image, given by (7), is kept within acceptable limits in each stage the final image can be formed in a vastly reduced number of operations. D_L is the length of a sub-aperture, D_M is the azimuth length of a sub image and R_{min} is the minimum distance from the synthetic aperture to the scene.

$$\dots(7)$$

$$|\Delta R|_{\max} \approx \frac{D_L D_M}{4 * R_{\min}}$$

The larger the error, the faster the image is produced and the lower the quality. The image is completely destroyed if this error is greater than $\lambda/4$ however. The speed of the algorithm is heavily affected by the choice of factorisations and number of stages, along with the approximation chosen and the physical dimensions of the scene. It is suggested in [5] that a suitable number of stages for radar imagery is around 3. For the sonar system used in this work the optimum number of stages required can be up to 6 depending on the image and aperture geometry. A simple program has been written to choose the optimum number of stages and factorisations for a given image and aperture geometry. The program works by predicting the computation time for all image and aperture combinations from 1 stage to 10 stages; although crude the best factorisations are found within 0.1 seconds.

The images shown in this paper have been produced using linear interpolation in range. The algorithm has been implemented using spline interpolation also. Using spline interpolation, the computation time and memory requirements are doubled and the improvement in image quality is small. Nearest neighbour interpolation is used in angle (for the polar images). It is highly likely that a more sophisticated interpolation scheme would improve image quality for very low approximations at the expense of increased computation time.

The memory requirements of FFBP can be made to be very low; if implemented carefully the memory requirements are not vastly more than twice that needed to store the final image (assuming the raw data is stored as a file and not in RAM and that memory for the final image is allocated only at the last stage of processing). At any point only two stages need to be stored in memory: the current stage and the previous stage. The implementation, in C, allocates memory for sub images only when it is required, and deletes subimages from the previous stage as soon as they are no longer required. Depending on the choice of the number of pixels in the intermediate sub images, the memory for each stage can be made to be similar to that of the final image.

5. RESULTS

This section presents the results of applying FFBP to synthetic aperture sonar data. The data was formed using a 10m rail mounted SAS system. DPCA [4] estimates of sway, surge and yaw were used for all images. Two targets, a 1m sphere and a cylinder, were placed at 70m from the rail. Figure 5 (a) shows the whole area of seabed visible to the sonar system. The image is 40m wide (azimuth) and 30m in range; note the rail was only 10m long. The maximum squint angle is around 20 degrees.

Figure 5 (b) shows the area of the scene containing the targets produced using FFBP using an approximation of $\lambda/18$ produced in 2 minutes. Figure 5 (c) shows the same area of seabed imaged using FFBP but with an approximation of $\lambda/60$ produced in 4 minutes 30 seconds. Figure 5 (d) shows the same image produced using the exact algorithm; computation time was 3 hours 45 minutes, around 110 times longer than using a $\lambda/18$ approximation. The algorithm was coded in C and compiled using the GNU gcc compiler with -O3 optimisation. It was run on a Pentium II 450 MHz machine running Linux kernel 2.4. The computation times for FFBP are in general similar to those of Fourier based methods such as the Range Doppler algorithm when forming images of similar sizes / resolutions. FFBP has the additional ability to produce images of different areas of seabed in correspondingly shorter times, and images with varying pixel size.

Title:
Graphics produced by IDL
Creator:
IDL Version 5.4 (linux x86)
Preview:
This EPS picture was not saved
with a preview included in it.
Comment:
This EPS picture will print to a
Post Script printer, but not to
other types of printers.

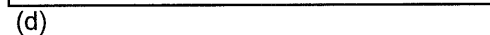
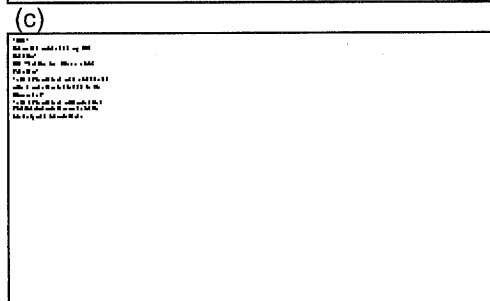
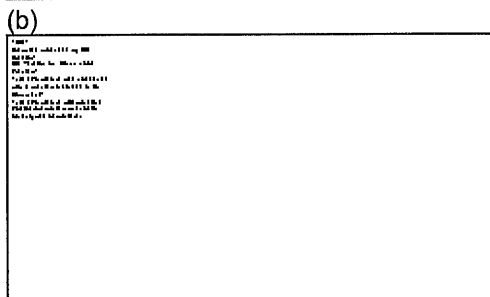
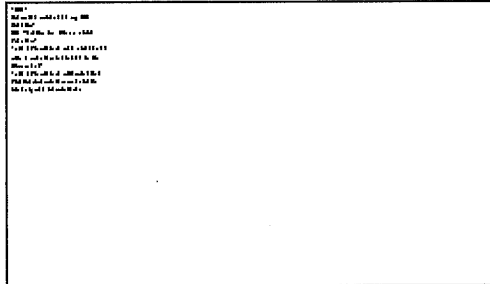


Figure 5 Images made using real sonar data (provided by QinetiQ Bincleaves). (a): Low resolution image of whole scene, approximation $\lambda/50$, (b): High resolution image of targets (1024*768 pixels) $\lambda/18$ approximation, computation time 2 mins., (c): same as (b) with $\lambda/60$ approximation, computation time 4 min. 20 sec. (d) exact method, computation time 3 hrs. 45 min.

The image with a large approximation is marginally more noisy than the image with a smaller approximation; this can be seen by looking at the shadowed areas. The difference between the images produced using an approximation of $\lambda/60$ and using the exact method is imperceptible, however the computation time is still very much less using FFBP.

6. CONCLUSIONS

This paper has shown that FFBP provides a means of producing SAS images in a similar time to frequency domain methods, whilst retaining the flexibility of a time domain method in terms of being able to form images of arbitrary sizes and resolutions and coping with a general aperture geometry. Although reduced computation time is achieved at the expense of making an approximation, if this variable approximation is made small the difference in image quality between the exact method and FFBP is imperceptible. The computation time is related to many factors including the synthetic aperture geometry and the size of the image produced. For a typical sonar image FFBP is around 100 times faster than the exact time-domain method. Although developed originally for SAR, FFBP has proved to be highly suited to SAS imaging. Because FFBP can be made to form an image a ping at a time it is likely to be suitable for use in any future developments of a real-time SAS system.

7. ACKNOWLEDGEMENTS

The algorithm was initially applied to sonar (for this work) by the principal author at the SACLANT Undersea Research Centre, La Spezia, Italy. Marc Pinto is gratefully acknowledged for suggesting and supervising the initial work, along with Andrea Bellettini and R. Hollet. Further development has been carried out at UCL. T. Sutton (UCL) is acknowledged for providing advice and computation times for the Range Doppler algorithm. The work of S. Chapman (QinetiQ Bincleaves) and team is acknowledged for providing the sonar data presented in this paper. L. Ulander (Swedish Defence Research Establishment) is very gratefully acknowledged for providing [5] (unpublished at the time of writing this paper).

8. REFERENCES

- [1] R. Raney, H. Runge and R. Bamler. 'Precision SAR Processing Using Chirp Scaling'. *IEEE Trans. on Geoscience and Remote Sensing*, 32:786-799, July 1994.
- [2] R. Balmer. 'A Comparison of Range-Doppler and Wavenumber Domain SAR Focusing Algorithms'. *IEEE Trans. on Geoscience and Remote Sensing*, 30:706-713.
- [3] L. Ulander, H. Hellsten, G. Stenstrom, 'Synthetic Aperture Radar Processing Using Fast Factorised Backprojection', in *EUSAR 2000 3rd European Conference on Synthetic Aperture Radar, Munich, Germany, 23-25 May 2000*, pp753-756, .
- [4] A. Bellettini and M. Pinto. 'Experimental Investigation of Synthetic Aperture Sonar Micronavigation', in *Underwater Acoustics ECUA 2000 5th European Conference on Underwater Acoustics, Lyon, France, July 2000*, vol. 1 pp445-450.
- [5] L. Ulander, H. Hellsten and G. Stenstrom, 'Synthetic-Aperture Radar Processing using Fast Factorised Back-Projection', submitted to: *IEEE Transactions on Aerospace and Electronic Systems* on 8 December 2000.
- [6] O. Seger, M. Herberthson and H. Hellsten, 'Real Time SAR Processing of Low Frequency Ultra Wide Band Radar Data', in *Proc. EUSAR '98 European Conference on Synthetic Aperture Radar Friedrichshafen, Germany, 25-27 May 1998*, pp489-492
- [7] S. Xiao, D. Munson Jr, S. Basu and Y.Bresler. 'An $N^2 \log N$ back-projection algorithm for SAR image formation', in *Conference Record of the Thirty-Fourth Asilomar Conference on Signals, Systems and Computers 2000*, vol. 1 pp3-7.
- [8] M. Skolnik, Radar Handbook, *McGraw-Hill Book Company*, 1970
- [9] C. A. Wiley, 'Pulse Doppler radar methods and apparatus', US Patent No. 3,196,436, 1954.
- [10] L. J. Cutrona, 'Comparison of sonar system performance achievable using synthetic aperture techniques with performance achievable using more conventional means.', *J. Acoust. Soc. Am.*, Aug. 1975, 58, (2) pp. 336-348
- [11] H. D. Griffiths, T.A. Rafik, Z.Meng, C.F.N. Cowan, H. Shafeeu, D.K. Anthony, 'Interferometric synthetic aperture sonar for high-resolution 3-D mapping of the seabed', *IEEE Proc.-Radar, Sonar Navig.*, Vol. 144, No. 2, April 1997.
- [12] S. M. Banks, A. Bellettini, 'The Application of Fast Factorised Back-Projection to Synthetic Aperture Sonar', *Internal report IN-686*, SACLANT Undersea Research Centre, La Spezia, Italy.

[1] Data has been provided by Thales Underwater Systems and QinetiQ Bincleaves.

[2] In squint and spotlight SAR the beam is steered by the application of appropriate delays to the channels to view areas of the scene not at boresight.

[3] The transmitter and receiver are assumed to be collocated at a position halfway between the two termed the *phase centre*.

